

PixCLIP: Achieving Fine-grained Visual Language Understanding via Any-granularity Pixel-Text Alignment Learning

Yicheng Xiao^{1,2*}, Yu Chen^{1,2*}, Haoxuan Ma^{3*}, Jiale Hong⁴, Caorui Li⁵, Lingxiang Wu^{1,2}, Haiyun Guo^{1,2}, Jinqiao Wang^{1,2†}

¹CASIA, ²UCAS, ³NJU, ⁴SJTU, ⁵SEU

Abstract

While the Contrastive Language-Image Pretraining (CLIP) model has achieved remarkable success in a variety of downstream vision language understanding tasks, enhancing its capability for fine-grained image-text alignment remains an active research focus. To this end, most existing works adopt the strategy of explicitly increasing the granularity of visual information processing, e.g., incorporating visual prompts to guide the model focus on specific local regions within the image. Meanwhile, researches on Multimodal Large Language Models (MLLMs) have demonstrated that training with long and detailed textual descriptions can effectively improve the model’s fine-grained vision-language alignment. However, the inherent token length limitation of CLIP’s text encoder fundamentally limits CLIP to process more granular textual information embedded in long text sequences. To synergistically leverage the advantages of enhancing both visual and textual content processing granularity, we propose PixCLIP, a novel framework designed to concurrently accommodate visual prompt inputs and process lengthy textual descriptions. Specifically, we first establish an automated annotation pipeline capable of generating pixel-level localized, long-form textual descriptions for images. Utilizing this pipeline, we construct LongGRIT, a high-quality dataset comprising nearly 1.5 million samples. Secondly, we replace CLIP’s original text encoder with the LLM and propose a three-branch pixel-text alignment learning framework, facilitating fine-grained alignment between image regions and corresponding textual descriptions at arbitrary granularity. Experiments demonstrate that PixCLIP showcases breakthroughs in pixel-level interaction and handling long-form texts, achieving state-of-the-art performance on fine-grained pixel-level tasks, while retaining the capabilities of original CLIP in handling global-level vision-language tasks.

Code — <https://github.com/StuHude/PixCLIP/>

Introduction

Contrastive Language-Image Pretraining (CLIP) (Radford et al. 2021) is a multimodal model that jointly trains image and text encoders via contrastive learning to align their features in a shared semantic space. Its features aim to capture all the semantic details within images, demonstrating strong

representation capabilities and exceptional generalizability. This inherent versatility makes them suitable for a variety of downstream tasks, such as open-world recognition (Chen et al. 2023; Zhou, Loy, and Dai 2022; Lan et al. 2024), retrieval (Huang et al. 2024; Saito et al. 2023; Zhang et al. 2024) and Multimodal Large Language Models (MLLMs) (Liu et al. 2023; Yang et al. 2024b).

Although CLIP captures the content of the entire image, focusing on regions of interest is crucial for achieving a more refined understanding. Traditional image processing techniques, such as cropping regions or masking irrelevant parts of images, tend to destroy and overlook contextual information. As a result, recent works have focused on enhancing the regional representation of CLIP, enabling it to accept visual prompts that guide attention to specific regions of interest. VisionLLM v2 (Wu et al. 2024a), ControlMLLM (Wu et al. 2024b), and Ferret (You et al. 2023) have introduced prompt encoders to enable multimodal models to receive visual prompt inputs, but these models cannot directly obtain visual representations to perform tasks such as retrieval. CLOC (Chen et al. 2025a) achieves alignment through a large number of bounding box-text pairs. However, its capability is limited to bounding boxes, not masks, and thus fails to capture the fine-grained, pixel-level details that masks can offer. Alpha CLIP (Sun et al. 2024) has addressed these issues by adding an alpha channel and using mask-text pairs for contrastive learning. However, since the training focused primarily on short and concise captions, these methods tend to struggle with longer and more detailed textual descriptions, performing poorly on tasks that require fine-grained analysis. So, is it possible to build a model that overcomes the limits to accept visual prompts for local regions and complex long texts, achieving image-text alignment at arbitrary granularity?

In this paper, we propose PixCLIP, a universal CLIP model for fine-grained understanding through any-granularity pixel-text alignment learning, as shown in Fig.1.1. We innovatively perform pixel-level semantic alignment between masks and complex long texts. After fine-tuning, the model can dynamically embed any local region of an image and align it with complex texts of arbitrary length. PixCLIP achieves a breakthrough in both the visual and textual domains, surpassing traditional granularity limits, and establishes itself as a more fine-grained foundational

*These authors contributed equally.

†Corresponding Author

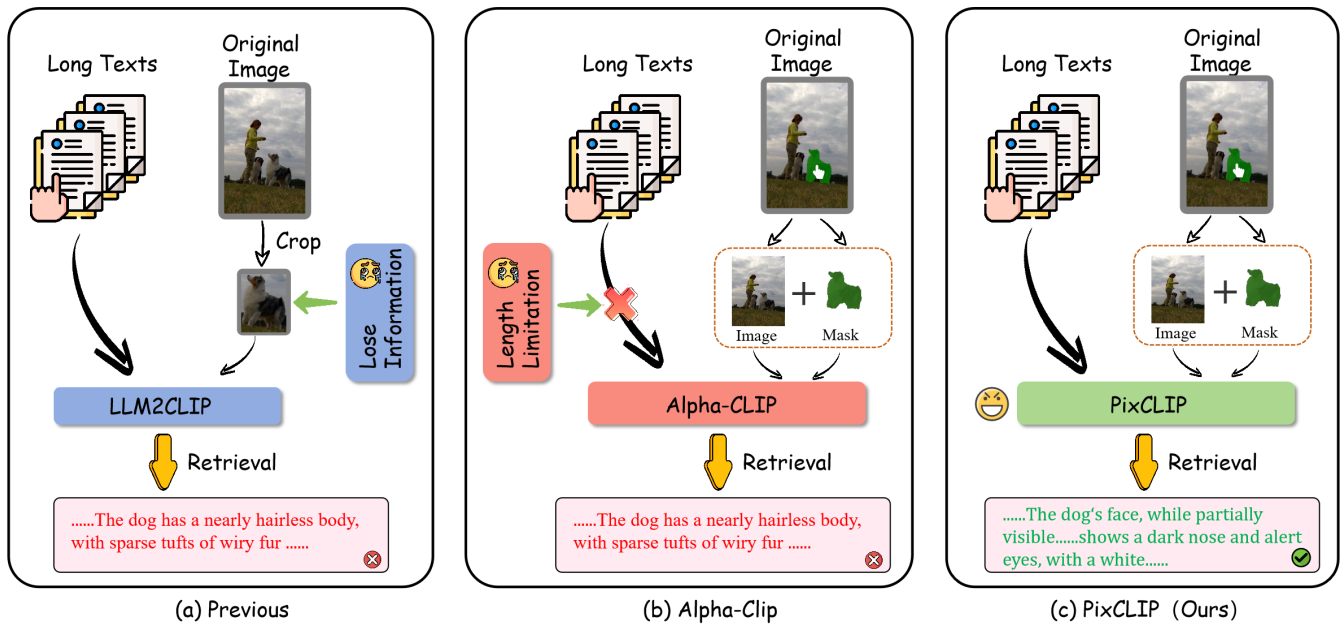


Figure 1: As shown on the (a), prior methods fail on fine-grained local tasks due to inability to accept mask input, While existing promptable methods struggle to handle long texts due to token limitations, as shown in (b). Only our method succeeds in yielding robust embeddings for image and text at any granularity.

model.

Specifically, existing mask-text datasets like GRiT (Peng et al. 2023) and FERRET (You et al. 2023) are limited by short text and a lack of large-scale, well-aligned training data. To address this, we first propose **LongGRIT**, an automatically generated dataset of 1.5 million image-local fine-grained expressions designed to boost model performance. We also utilized 2,000 masked regions from LongGRIT to benchmark existing models for fine-grained local mask-text retrieval in complex settings, uncovering significant opportunities for improvement and further research.

Secondly, we propose a multi-grained alignment framework. (1) We use an LLM as the text encoder and then employ contrastive learning with mask-text pairs. This enables the model to directly obtain embeddings from images with mask and align them with fine-grained text features. (2) In parallel, we utilize Fine-grained Cropping Alignment. This branch extracts features solely from the region indicated by the mask. It aims to make these features more similar to the features from the first step, thereby enhancing the features to concentrate more strongly on the masked region. (3) Simultaneously, in the Local-Global Representation Enhancement branch, the mask covers the whole image, equivalent to extracting whole-image features and then mutually enhances the initial mask embedding by features from the corresponding region, jointly optimizing the representation capabilities for both the global and local.

We conduct extensive experiments on RefCOCO (Lin et al. 2015), Ref-SAV (Yuan et al. 2025), Instance-COCO (Lin et al. 2015), ImageNet-S (Gao et al. 2023) for region-level evaluation, as well as a series of image-text retrieval datasets such as DOCCI, Urban, and Flickr. The results demonstrate that our model successfully enables the pro-

cessing of complex long texts while maintaining the ability to accept local visual cues, greatly improving the performance of fine-grained tasks.

Our contribution is threefold:

1. We propose PixCLIP, a universal foundation model that extends the input to any local region and long texts. Extensive experiments demonstrate the superiority of this model in both region-level tasks and traditional tasks.
2. We construct and release the LongGRIT dataset, which contains 1.5 million detailed mask descriptions automatically generated and validated by SOTA MLLMs.
3. We propose a three-branch pixel-text alignment learning framework that significantly enhances the model’s performance through fine-grained cropping and local-global enhancement.

Related Works

Localized Image Representation

To enable CLIP to disentangle regions from the whole image for more targeted processing and understanding, various methods have been explored in the field of segmentation. MaskCLIP (Zhou, Loy, and Dai 2022) and ODISE (Xu et al. 2023) use attention masks to make CLIP focus more on local regions. Another approach is to change the input image by simply cropping or masking the image to leave only the foreground object. ReCLIP (Subramanian et al. 2022) and OvarNet (Chen et al. 2023) crop the original image using bounding box from object proposal network. However, the valuable context information is lost except for using complex post-process proposed in ReCLIP (Subramanian et al. 2022). Some other approaches prompt the CLIP by modifying the input image, guiding CLIP to focus on the area of in-

terest. For example, Red-Circle (Shtedritski, Rupprecht, and Vedaldi 2023), FGVP (Yang et al. 2023) use a circle or mask contour to tell CLIP where to focus. But the direct modification of images causes a domain gap with CLIP pertaining images. Alpha-CLIP (Sun et al. 2024) incorporates an additional alpha channel, which proved that it is a more potential paradigm.

Enabling Long Text for CLIP

It has been widely recognized that the quality of CLIP’s text embedding is coarse and limited to only 77 tokens. Many works have attempted to extend the length of CLIP captions and retrain CLIP accordingly. DreamLIP (Zheng et al. 2024) leveraged ShareCaptioner (Chen et al. 2024) and Instruct-BLIP to augment 30M captions. LongCLIP processes long text by encoding chunks and aggregating them again. These methods were compromised by splitting captions into multiple shorter segments (Zheng et al. 2024; Fan et al. 2023), or fine-tuning the positional encoding to support longer token inputs (Zhang et al. 2024). Recent work LLM2CLIP (Huang et al. 2024) also explores aligning fine-tuned LLM with vision encoder directly. Our model uses LLM as the text encoder and successfully supports the ability for any-granularity visual representation while supporting long text inputs.

Region-level image annotation

CLIP is pretrained on large-scale datasets like LAION-400M (Schuhmann et al. 2021) and LAION-5B (Schuhmann et al. 2022), while fine-grained pixel-level labels are not available due to high manual labor costs. CLOC (Chen et al. 2025a) also generates fine-grained text labels via the pseudo-labeling pipeline. However, its data format is limited to box and cannot achieve pixel-level annotation, namely mask. Alpha-CLIP uses SAM (Kirillov et al. 2023) and BLIP (Li et al. 2022) to generate 20M object-level caption. But their local captions are either segmented from the entire image caption or generated by the clip-based captioning model, resulting in: (1) It is difficult to ensure the quality of data; (2) All region caption are only composed of several words, with limited length and insufficient fine-grained information. We proposed a fine-grained region-level image annotation framework, which obtained a large number of high-quality fine-grained long texts and region pairs from **multiple perspectives**, by using **multiple state-of-the-art MLLMs** and undergoing **multiple verifications**.

Method

Fine-grained Data Generation

As illustrated in Fig.3, our pipeline builds upon the GRIT-20M (Peng et al. 2023) dataset and consists of three stages: Object-level expression annotation, Context-level expression annotation, and Fine-grained expression annotation. Each stage progressively refines the target object’s description, from appearance attributes to spatial context, culminating in a detailed referring expression.

Object-level expression annotation. Initially, we isolate each object using its segmentation mask from GRIT-20M.

Both the cropped object and its mask are fed into InternVL2-76B (Chen et al. 2025b) to generate an initial *object-level* caption focused on visual attributes (e.g., shape, color, texture). To ensure semantic consistency, we employ Qwen2-72B (Yang et al. 2024a) to validate the caption against the original image. Any captions flagged as inconsistent (e.g., describing non-existent features) or semantically invalid (e.g., "a red clock" for a blue vase) are discarded, while valid captions are retained as *object-level* annotations.

Context-level expression annotation. In this stage, we input the original image and the object’s bounding box into Griffon-G-26B (Zhan et al. 2024), a vision-language model specialized in spatial reasoning. The model generates a *context-level* caption that describes the object’s location (e.g., "leftmost on the mantelpiece") and its relationship to surrounding objects. This complements the object-level caption by capturing contextual information in the first stage.

Fine-grained expression annotation. Finally, we integrate the object-level and context-level captions through DeepSeek-R1-70B (DeepSeek-AI et al. 2025), which synthesizes both inputs into a unified *fine-grained* expression. For example, if the object-level caption states "a decorative lantern" and the context-level caption notes "the leftmost object on a mantelpiece," DeepSeek-R1-70B merges these into: "The object is a decorative lantern with intricate carvings, positioned as the leftmost item on a wooden mantelpiece flanked by framed portraits." This hierarchical approach ensures descriptions are both precise and contextually grounded.

Model structure

Our PixCLIP implements subtle structural modifications to the CLIP image encoder to preserve CLIP’s prior knowledge. Similar to how an image is encoded by a patch embedding layer in vision transformers (ViTs) (Dosovitskiy et al. 2021), we introduce a paralleled mask patch embedding layer to takes in 2D inputs with one channel. We process the input images and masks separately through respective patch embedding layers, then sum their outputs. Specifically, for the inputs images I and Masks M , we have the feature F :

$$F = E_n(\text{Conv}_I(I) + \text{Conv}_M(M) + P) \quad (1)$$

where $\text{Conv}_I(\cdot)$ and $\text{Conv}_M(\cdot)$ are the image and mask patch embedding layer. Correspondingly, E_n is the vision encoder and P denotes the positional encoding. The newly added mask embedding layer $\text{Conv}_M(\cdot)$ is initialized to output zeros, ensuring that the model’s initial behavior is unaffected prior to fine-tuning.

Multi-granularity Training method

Overview. PixCLIP employs three main alignment strategies: global image-text alignment, local mask-text alignment, and multi-scale feature enhancement. As depicted in Fig.2, PixCLIP adopts the architecture likes CLIP, which consists of the vision encoder V and the language encoder L , but employs more complex inputs and objectives. We initialized the ViT weights from LLM2CLIP (Huang et al. 2024) and use LLAMA3-8B (Grattafiori et al. 2024) as our text

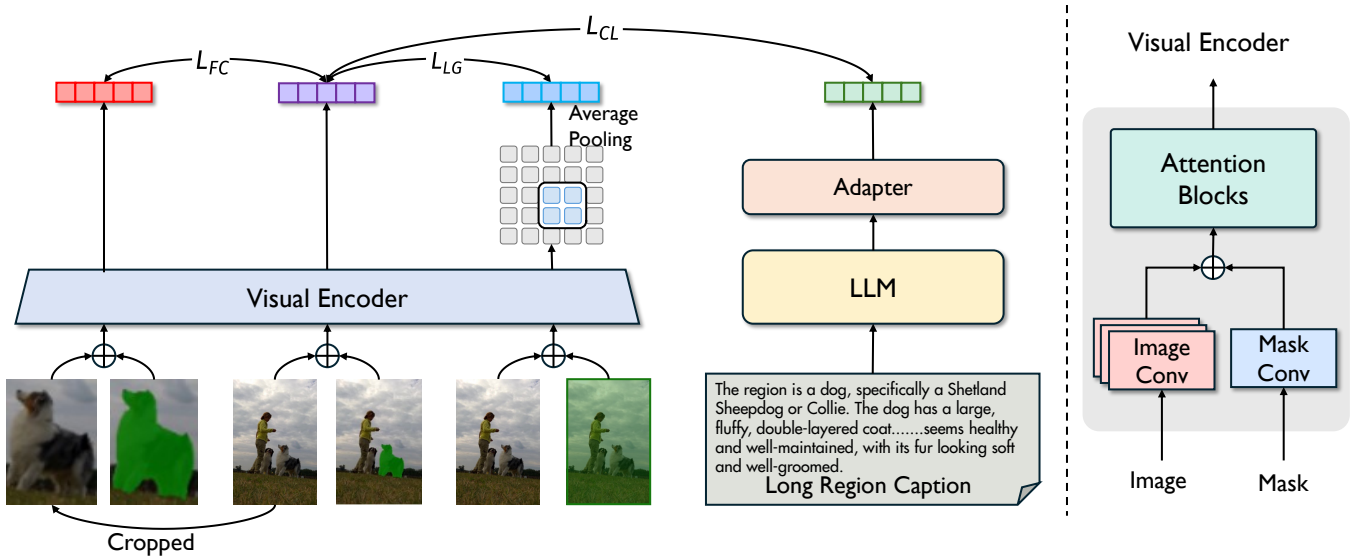


Figure 2: The framework of the proposed PixCLIP. Our model structure allows for inheriting weights from existing model and we propose the Fine-grained Cropping Alignment and Local-Global Representation Enhancement branches to enhance the mask-based visual embeddings.

encoder to receive long text input and leverage the open-world knowledge of LLM. Inheriting weights of LLAMA3-8B and the adaptor (a simple projector) from LLM2Vec (BehnamGhader et al. 2024), we first make self-supervised fine-tuning (BehnamGhader et al. 2024) on our text data following its setting and then freezing it as the text tower to reduce training overhead. For training, each input batch consists of \mathcal{B} samples. The input includes an original image I_i , a mask M_i , and a long text T_i describing the masked region. Additionally, from the original image I_i and mask M_i , we generate a *cropped image* I'_i that tightly contains the masked region M_i , and a mask M'_i outlining the object within the cropped image I'_i , as illustrated in Figure 3. Thus, the full input for sample i is the tuple $(I_i, M_i, T_i, I'_i, M'_i)$. The long texts T_i are sourced from our LongGRIT dataset.

Mask-text contrastive learning. We basically following the previous CLIP-based settings. For the inputs image and masks $\{I_i, M_i\}$, PixCLIP first encodes them to produce a visual embedding e_v which is focused on the local region referred to by the mask. And LLM encodes the long text to text embedding e_t , the cosine similarity is calculated as:

$$S(\mathbf{e}_v, \mathbf{e}_t) = \frac{\mathbf{e}_v \cdot \mathbf{e}_t}{\|\mathbf{e}_v\| \|\mathbf{e}_t\|} \quad (2)$$

Model is forced to learn visual and text embedding by maximizing the cosine similarity to the corresponding text and image embeddings, while minimizing the cosine similarity to other non-corresponding ones in the batch:

$$L_{CL}(\mathbf{e}_v, \mathbf{e}_t) = -\frac{1}{2\mathcal{B}} \sum_{i=1}^{\mathcal{B}} \left(\log \frac{\exp(S(\mathbf{e}_v^i, \mathbf{e}_t^i)/\tau)}{\sum_{j=1}^{\mathcal{B}} \exp(S(\mathbf{e}_v^i, \mathbf{e}_t^j)/\tau)} + \log \frac{\exp(S(\mathbf{e}_t^i, \mathbf{e}_v^i)/\tau)}{\sum_{j=1}^{\mathcal{B}} \exp(S(\mathbf{e}_t^i, \mathbf{e}_v^j)/\tau)} \right) \quad (3)$$

Following previous work (Sun et al. 2024), we set a 10% ratio to occasionally set the mask to all 1 (representing the full image) to maintain the global embedding ability for the entire image. When it occurs, the text is changed to the whole image caption for global alignment.

Fine-grained cropping alignment. Some prior methods extract local features from global image representations, often leading to loss of fine-grained details—particularly for small objects in complex scenes. Therefore, to enhance features that are more focused on the region indicated by the mask, on another branch, we cropped the region corresponding to the mask. The cropped region tightly encloses the mask, making the content within the mask the primary focus of the image. After being enlarged, the embedding v_c, t_c obtained from the cropped image I_c and M_c via the visual encoder is aligned with the original visual embedding, to force the model to focus more on the visual details themselves:

$$L_{FC} = L_{CL}(v_c, t_c) \quad (4)$$

Since we want the main embedding to also retain contextual interaction and boundary information, a full alignment with the embedding from the cropped detailed mask is not appropriate. We can only maintain the positive sample matching relationship. This method can also prevent poor model training, keeping the model from focusing too much on the whole image when a mask is provided as input.

Local-Global representation enhancement. A model's ability to understand the whole image and its local regions is complementary, meaning their optimization directions tend to converge. A correct global understanding of an image, in fact, stems precisely from the cumulative accurate understanding of all its local regions. This, in turn, dictates whether the model's contextual comprehension of any arbitrary local area is accurate. Therefore, we utilize a branch

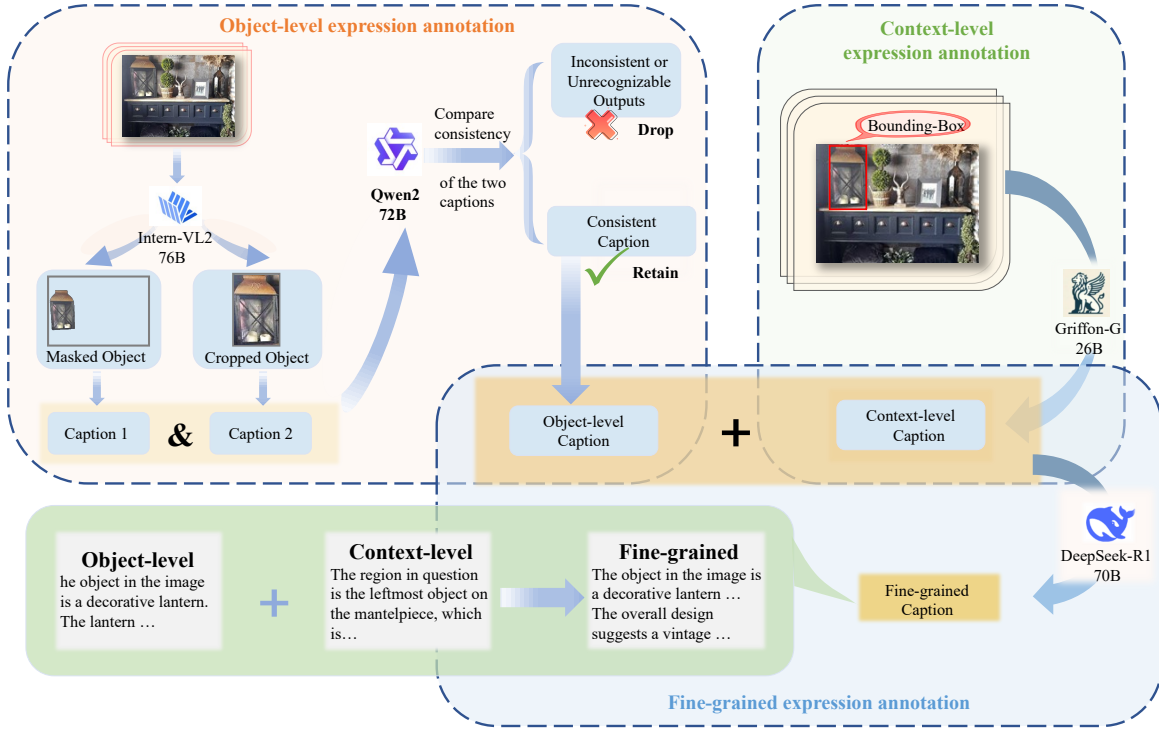


Figure 3: The pipeline of our data generation method. Using multiple MLLMs, we generate object captions and in-context captions. They are then checked and merged into fine-grained captions for use in further training stage.

to explicitly connect these two aspects, combining them into a joint learning task. This branch enables the model to maintain its full-image capabilities and further explore the deep relationship between comprehensive image understanding and arbitrary local comprehension, ensuring both are optimized synergistically.

Specifically, on another branch, we input the original image I with an all-1 mask M_1 . From the global dense representation, we extract local representations once more. Specifically, regional visual representations f'_v are extracted by pooling visual dense features $\{f_v^i\}_{i \leq \mathcal{P}}$ according to the region occupied by the mask M , using Average Pooling:

$$f'_v = \text{proj} \left(\text{AvgPool} \left(\{f_v^i \mid p_i \in \mathcal{M} \cap \mathcal{P}, \frac{|\mathcal{M} \cap \mathcal{P}|}{|\mathcal{P}|} > \tau \} \right) \right) \quad (5)$$

$$L_{LG} = L_{CL}(f'_v, f_v) \quad (6)$$

Then the self-supervision process can continuously update and improve itself.

Finally the total loss is calculated as:

$$L = L_{CL} + \alpha L_{FC} + \beta L_{LG} \quad (7)$$

Noted that throughout the entire training process, short texts are also included and trained together with long texts, in order to enhance the model's robustness.

Experiment

Experimental Setting

Our experiments evaluated PixCLIP's metrics across multiple dimensions. For evaluation, we used ViT-B/16 models. Our models were trained on the LongGRIT dataset we made. The batch size was 1024 for ViT-B/16, the α and β is set to 0.25. The entire training was completed on 8 H20 100G, totaling 8 epochs.

We compared our approach to previous state-of-the-art (SOTA) models on both pixel-level regional tasks and traditional image-level tasks. For regional tasks, we selected previous works that focused on adapting CLIP for specific areas, including MaskCLIP (Zhou, Loy, and Dai 2022), MaskAdaptedCLIP (Liang et al. 2023), Red Circle (Shtedritski, Rupprecht, and Vedaldi 2023), Alpha-CLIP (Sun et al. 2024), and so on. We were unable to compare our method with CLOC (Chen et al. 2025a) as it has not yet open-sourced its model. In traditional image-text retrieval, our method showed strong performance on both short- and long-text datasets, outperforming models specifically designed for long-text retrieval, such as LongCLIP (Zhang et al. 2024) and LLM2CLIP (Huang et al. 2024).

PixCLIP in Region Recognition

Zero-shot region classification. We firstly evaluate our model in ImageNet-S (Gao et al. 2023) dataset for zero-shot classification analysis, which comprises 919 classes with semantic segmentation annotations selected from ImageNet-1k. The result is shown as Table.7:

Methods	Input type	top1	top5
CLIP(Radford et al. 2021)	Crop Image	66.48%	88.90%
MaskedAdaptedCLIP(Liang et al. 2023)	Crop Image	57.86%	79.12%
Red Circle(Shtedritski, Rupprecht, and Vedaldi 2023)	Visual Prompt	65.37%	88.68%
MaskCLIP(Zhou, Loy, and Dai 2022)	Visual Prompt	67.86%	89.40%
Alpha-CLIP (Sun et al. 2024)	Visual Prompt	68.89%	90.51%
PixCLIP	Visual Prompt	69.57%	91.17%

Table 1: Accuracy comparison of Zero-shot classification results on ImageNet-S. All methods use ViT-B/16.

Methods	RefCOCO		RefCOCO+		RefCOCog
	Val	Test	Val	Test	
CPT(Yao et al. 2022)	32.2	36.1	31.9	35.2	36.7
ReCLIP(Subramanian et al. 2022)	45.8	46.1	47.9	50.1	59.3
Red Circle(Shtedritski, Rupprecht, and Vedaldi 2023)	49.8	58.6	55.3	63.9	59.4
Alpha-CLIP (Sun et al. 2024)	55.7	61.1	55.6	62.7	61.2
PixCLIP	59.93	69.9	59.1	68.5	61.8

Table 2: Performance on RefCOCO+/g Datasets. All models use ViT-B/16.

Methods	Zero-shot Classification	
	Top1	Top5
CLIP(Radford et al. 2021)	64.21%	86.69%
Alpha-CLIP (Sun et al. 2024)	71.08%	88.90%
LLM2CLIP (Huang et al. 2024)	70.16%	87.40%
PixCLIP	76.68%	90.56%

Table 3: Accuracy comparison on Instance-COCO. All methods use ViT-B/16.

For scenarios that need to crop or mask objects in images (Subramanian et al. 2022; Chen et al. 2023). Previous work (Sun et al. 2024) has conducted classification tests for in such scenarios using the validation set of the Instance-COCO (Lin et al. 2015) dataset, which consists of 80 classes. We followed the setting to crop objects using ground-truth bounding boxes and enlarged them by 1.5 times (referred to as coco crop). The experimental results are as Table.8. Importantly, CLIP and LLM2CLIP take the cropped images directly as input.

Zero shot REC(referring expression comprehension). For the REC task, we conducted experiments on Ref-COCO(Lin et al. 2015), RefCOCO+(Lin et al. 2015), and RefCOCog(Lin et al. 2015). Following the setup of Alpha CLIP, we used object proposals predicted by a pretrained detector (Yu et al. 2018) and employed SAM to obtain masks for each proposal. On this task, we significantly outperformed the previous SOTA.

PixCLIP in Multi-modal Retrieval.

As a CLIP-like multimodal foundation model, we meticulously evaluated PixCLIP’s performance on cross-modal retrieval tasks. This evaluation included multiple traditional image-text retrieval benchmarks to assess our model’s retention of holistic image understanding, alongside our newly

extended pixel-level benchmark: Mask and Text Retrieval. Experimental results clearly show PixCLIP delivers state-of-the-art (SOTA) performance, whether dealing with full images or localized regions, and whether processing concise or extended text descriptions.

Traditional Retrieval with Full-Image and Text. For short-text retrieval, we used the MSCOCO (Lin et al. 2015) 5K test set and the Flickr (Young et al. 2014) 1K test set. For long-text retrieval, we employed datasets from Long-CLIP, including a 1K subset of ShareGPT4V (Chen et al. 2024), the Urban1K (Zhang et al. 2024) dataset, and the DOCCI (Onoe et al. 2024) dataset. The ShareGPT4V-1M dataset consists of captions generated using GPT-4V and ShareCaptioner, covering images from LAION, CC, SBU (Ordonez, Kulkarni, and Berg 2011), and MS COCO. Urban1K includes captions for 1,000 urban scene images, each richly annotated with detailed descriptions. DOCCI contains 1.5K high-resolution images with human-annotated captions and was used for retrieval evaluation. Results are shown as Table.4 and Fig.4.

Pixel-level Retrieval with Mask and Text. Ref-SAV (Yuan et al. 2025) is a dataset originally intended for video referring segmentation. Ref-SAV includes 70,000 masklets and corresponding long captions, with an average caption length of over 100 words, providing fine-grained details. Although initially designed for video referring segmentation, we found it particularly well-suited for evaluating our model’s performance. We extracted 1,000 mask-text samples for retrieval and compared our work with the previous SOTA work Alpha-CLIP. Our work significantly outperforms Alpha-CLIP in performance. This is primarily due to our LLM’s ability to better extract fine-grained text features from longer captions, a capability fundamentally lacking in Alpha-CLIP’s traditional text encoder.

Methods	Flickr30k		COCO		ShareGPT4V		Urban-1k		DOCCI		Average	
	I2T	T2I										
ALIGN	80.6	62.2	52.0	43.2	75.9	80.6	62.2	59.1	59.7	62.1	66.1	61.4
BLIP	80.6	74.1	61.7	48.5	65.8	74.3	45.5	48.5	50.5	53.5	60.8	59.8
Jina-CLIP	80.6	67.4	55.6	41.1	-	-	87.7	88.0	78.7	80.0	75.7	69.1
Long-CLIP	85.8	70.6	56.9	40.9	94.8	93.5	79.1	79.1	63.1	71.4	75.9	71.1
CLIP	82.3	62.2	52.4	33.1	84.5	79.8	67.5	53.1	60.7	57.1	69.5	57.1
EVA02	86.2	71.5	58.7	42.1	90.5	85.5	67.0	60.8	67.7	68.0	74.0	65.6
LLM2CLIP	88.5	78.0	63.6	49.8	98.0	98.1	84.7	89.7	85.5	86.8	84.1	80.5
PixCLIP	84.2	87.0	52.7	50.2	97.4	97.7	91.0	93.7	96.7	96.4	84.4	85.0

Table 4: Retrieval performance comparison on existing datasets.

Methods	M2T			T2M		
	Recall@1	Recall@5	Recall@10	Recall@1	Recall@5	Recall@10
Alpha CLIP(Sun et al. 2024)	28.3%	50.4%	59.9%	27.5%	46.9%	55.7%
PixCLIP	47.3%	66.4%	73.4%	47.9%	66.8%	74.1%

Table 5: Accuracy comparison on Zero-shot mask-to-text (M2T) and text-to-mask (T2M) results on Ref-SAV.

Models	Region Tasks			Full-Image Tasks	
	RefCOCO Val	Ref-SAV M2T	Ref-SAV T2M	Urban1k I2T	Urban1k T2I
LLM2CLIP(Huang et al. 2024)	-	-	-	84.7%	89.7%
L_{CL}	51.144%	47.0%	46.9%	87.1%	92.4%
$L_{CL} + L_{LG}$	59.041%	47.4%	47.3%	88.9%	93.2%
$L_{CL} + L_{LG} + L_{FC}$	59.926%	47.3%	47.9%	91.0%	93.7%

Table 6: The ablation results on both pixel-level and image-level tasks.

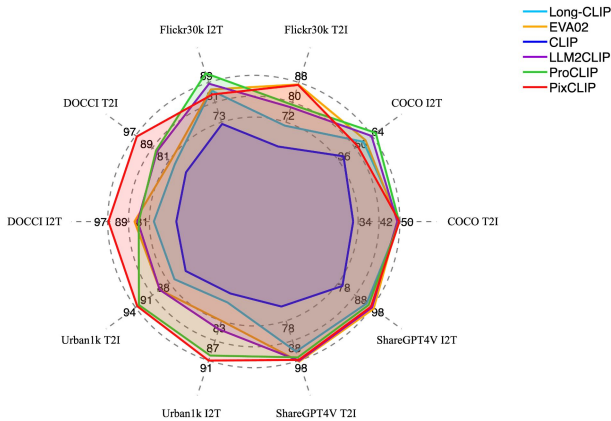


Figure 4: Retrieval comparison with previous models in traditional Image-Text benchmarks.

Ablation Experiment

The PixCLIP training objective consists of three components: L_{CL} , L_{FC} , L_{LG} . We conducted the ablation study on these components across both **regional-level tasks** (REC and mask-text retrieval on Ref-SAV) and **image-level tasks**.

Our experiments show that simply using direct align-

ment between mask-based visual features and text is inefficient, leading to poor performance and degradation on whole-image inputs. We hypothesize this is because, while the LLM provides rich text features, the limited amount of local data makes it challenging for the model to learn robust representations that work for both local and global visual inputs. The L_{FC} , L_{LG} successfully resolves this issue and significantly boosts performance.

This result precisely confirms the hypothesis we outlined in our method: a strong foundation model’s capability for regional and broad enhance each other.

Conclusion

In this paper, we propose PixCLIP, a model capable of accepting arbitrary local input on the image side indicated by a mask and processing text input of arbitrary length on the text side, to achieve deeper, multi-level image-text alignment. For significance, we are no longer limited to traditional monotonous image-text pairs, achieving perfect adaptation to arbitrary image pixels and long text sequences, thus being a more unified CLIP. For training, we propose a multi-grained alignment framework with two additional branches: Fine-grained Cropping Alignment and Local-Global Representation Enhancement, for performance enhancement. For

data, we engineered an automatic pipeline to construct a dataset of 1.5M masks with corresponding fine-grained captions, serving as a benchmark for mask-text retrieval tasks. We believe this research will facilitate further exploration in the multimodal domain.

References

- BehnamGhader, P.; Adlakha, V.; Mosbach, M.; Bahdanau, D.; Chapados, N.; and Reddy, S. 2024. Llm2vec: Large language models are secretly powerful text encoders. *arXiv preprint arXiv:2404.05961*.
- Chen, H.-Y.; Lai, Z.; Zhang, H.; Wang, X.; Eichner, M.; You, K.; Cao, M.; Zhang, B.; Yang, Y.; and Gan, Z. 2025a. Contrastive Localized Language-Image Pre-Training. arXiv:2410.02746.
- Chen, K.; Jiang, X.; Hu, Y.; Tang, X.; Gao, Y.; Chen, J.; and Xie, W. 2023. Ovaret: Towards open-vocabulary object attribute recognition. In *Proceedings of the IEEE/CVF conference on computer vision and pattern recognition*, 23518–23527.
- Chen, L.; Wei, X.; Li, J.; Dong, X.; Zhang, P.; Zang, Y.; Chen, Z.; Duan, H.; Lin, B.; Tang, Z.; Yuan, L.; Qiao, Y.; Lin, D.; Zhao, F.; and Wang, J. 2024. ShareGPT4Video: Improving Video Understanding and Generation with Better Captions. arXiv:2406.04325.
- Chen, Z.; Wang, W.; Cao, Y.; Liu, Y.; Gao, Z.; Cui, E.; Zhu, J.; Ye, S.; et al. 2025b. Expanding Performance Boundaries of Open-Source Multimodal Models with Model, Data, and Test-Time Scaling. arXiv:2412.05271.
- DeepSeek-AI; Guo, D.; Yang, D.; Zhang, H.; Song, J.; Zhang, R.; Xu, R.; Zhu, Q.; et al. 2025. DeepSeek-R1: Incentivizing Reasoning Capability in LLMs via Reinforcement Learning. arXiv:2501.12948.
- Dosovitskiy, A.; Beyer, L.; Kolesnikov, A.; Weissenborn, D.; Zhai, X.; Unterthiner, T.; Dehghani, M.; Minderer, M.; Heigold, G.; Gelly, S.; Uszkoreit, J.; and Houlsby, N. 2021. An Image is Worth 16x16 Words: Transformers for Image Recognition at Scale. arXiv:2010.11929.
- Fan, L.; Krishnan, D.; Isola, P.; Katabi, D.; and Tian, Y. 2023. Improving clip training with language rewrites. *Advances in Neural Information Processing Systems*, 36: 35544–35575.
- Gao, S.; Li, Z.-Y.; Yang, M.-H.; Cheng, M.-M.; Han, J.; and Torr, P. 2023. Large-Scale Unsupervised Semantic Segmentation. *IEEE Transactions on Pattern Analysis and Machine Intelligence*, 45(6): 7457–7476.
- Grattafiori, A.; Dubey, A.; Jauhri, A.; Pandey, A.; Kadian, A.; Al-Dahle, A.; Letman, A.; et al. 2024. The Llama 3 Herd of Models. arXiv:2407.21783.
- Huang, W.; Wu, A.; Yang, Y.; Luo, X.; Yang, Y.; Hu, L.; Dai, Q.; Dai, X.; Chen, D.; Luo, C.; et al. 2024. Llm2clip: Powerful language model unlock richer visual representation. *arXiv preprint arXiv:2411.04997*.
- Kirillov, A.; Mintun, E.; Ravi, N.; Mao, H.; Rolland, C.; Gustafson, L.; Xiao, T.; Whitehead, S.; Berg, A. C.; Lo, W.-Y.; Dollár, P.; and Girshick, R. 2023. Segment Anything. arXiv:2304.02643.
- Lan, M.; Chen, C.; Ke, Y.; Wang, X.; Feng, L.; and Zhang, W. 2024. Clearclip: Decomposing clip representations for dense vision-language inference. In *European Conference on Computer Vision*, 143–160. Springer.
- Li, J.; Li, D.; Xiong, C.; and Hoi, S. 2022. Blip: Bootstrapping language-image pre-training for unified vision-language understanding and generation. In *International conference on machine learning*, 12888–12900. PMLR.
- Liang, F.; Wu, B.; Dai, X.; Li, K.; Zhao, Y.; Zhang, H.; Zhang, P.; Vajda, P.; and Marculescu, D. 2023. Open-vocabulary semantic segmentation with mask-adapted clip. In *Proceedings of the IEEE/CVF conference on computer vision and pattern recognition*, 7061–7070.
- Lin, T.-Y.; Maire, M.; Belongie, S.; Bourdev, L.; Girshick, R.; Hays, J.; Perona, P.; Ramanan, D.; Zitnick, C. L.; and Dollár, P. 2015. Microsoft COCO: Common Objects in Context. arXiv:1405.0312.
- Liu, H.; Li, C.; Wu, Q.; and Lee, Y. J. 2023. Visual Instruction Tuning. arXiv:2304.08485.
- Onoe, Y.; Rane, S.; Berger, Z.; Bitton, Y.; Cho, J.; Garg, R.; Ku, A.; Parekh, Z.; Pont-Tuset, J.; Tanzer, G.; et al. 2024. Docci: Descriptions of connected and contrasting images. In *European Conference on Computer Vision*, 291–309. Springer.
- Ordóñez, V.; Kulkarni, G.; and Berg, T. 2011. Im2text: Describing images using 1 million captioned photographs. *Advances in neural information processing systems*, 24.
- Peng, Z.; Wang, W.; Dong, L.; Hao, Y.; Huang, S.; Ma, S.; and Wei, F. 2023. Kosmos-2: Grounding multimodal large language models to the world. *arXiv preprint arXiv:2306.14824*.
- Radford, A.; Kim, J. W.; Hallacy, C.; Ramesh, A.; Goh, G.; Agarwal, S.; Sastry, G.; Askell, A.; Mishkin, P.; Clark, J.; Krueger, G.; and Sutskever, I. 2021. Learning Transferable Visual Models From Natural Language Supervision. arXiv:2103.00020.
- Saito, K.; Sohn, K.; Zhang, X.; Li, C.-L.; Lee, C.-Y.; Saenko, K.; and Pfister, T. 2023. Pic2word: Mapping pictures to words for zero-shot composed image retrieval. In *Proceedings of the IEEE/CVF Conference on Computer Vision and Pattern Recognition*, 19305–19314.
- Schuhmann, C.; Beaumont, R.; Vencu, R.; Gordon, C.; Wightman, R.; Cherti, M.; Coombes, T.; Katta, A.; Mullis, C.; Wortsman, M.; Schramowski, P.; Kundurthy, S.; Crowson, K.; Schmidt, L.; Kaczmarczyk, R.; and Jitsev, J. 2022. LAION-5B: An open large-scale dataset for training next generation image-text models. arXiv:2210.08402.
- Schuhmann, C.; Vencu, R.; Beaumont, R.; Kaczmarczyk, R.; Mullis, C.; Katta, A.; Coombes, T.; Jitsev, J.; and Komatsuzaki, A. 2021. LAION-400M: Open Dataset of CLIP-Filtered 400 Million Image-Text Pairs. arXiv:2111.02114.
- Shtedritski, A.; Rupprecht, C.; and Vedaldi, A. 2023. What does clip know about a red circle? visual prompt engineering for vlms. In *Proceedings of the IEEE/CVF International Conference on Computer Vision*, 11987–11997.

- Subramanian, S.; Merrill, W.; Darrell, T.; Gardner, M.; Singh, S.; and Rohrbach, A. 2022. Reclip: A strong zero-shot baseline for referring expression comprehension. *arXiv preprint arXiv:2204.05991*.
- Sun, Z.; Fang, Y.; Wu, T.; Zhang, P.; Zang, Y.; Kong, S.; Xiong, Y.; Lin, D.; and Wang, J. 2024. Alpha-clip: A clip model focusing on wherever you want. In *Proceedings of the IEEE/CVF conference on computer vision and pattern recognition*, 13019–13029.
- Wu, J.; Zhong, M.; Xing, S.; Lai, Z.; Liu, Z.; Chen, Z.; Wang, W.; Zhu, X.; Lu, L.; Lu, T.; et al. 2024a. Vision-llm v2: An end-to-end generalist multimodal large language model for hundreds of vision-language tasks. *Advances in Neural Information Processing Systems*, 37: 69925–69975.
- Wu, M.; Cai, X.; Ji, J.; Li, J.; Huang, O.; Luo, G.; Fei, H.; Jiang, G.; Sun, X.; and Ji, R. 2024b. Controlmlm: Training-free visual prompt learning for multimodal large language models. *Advances in Neural Information Processing Systems*, 37: 45206–45234.
- Xu, J.; Liu, S.; Vahdat, A.; Byeon, W.; Wang, X.; and Mello, S. D. 2023. Open-Vocabulary Panoptic Segmentation with Text-to-Image Diffusion Models. *arXiv:2303.04803*.
- Yang, A.; Yang, B.; Hui, B.; Zheng, B.; Yu, B.; Zhou, C.; Li, C.; Li, C.; Liu, D.; Huang, F.; et al. 2024a. Qwen2 Technical Report. *arXiv:2407.10671*.
- Yang, L.; Wang, Y.; Li, X.; Wang, X.; and Yang, J. 2023. Fine-Grained Visual Prompting. *arXiv:2306.04356*.
- Yang, X.; Peng, Y.; Ma, H.; Xu, S.; Zhang, C.; Han, Y.; and Zhang, H. 2024b. Lever LM: configuring in-context sequence to lever large vision language models. *Advances in Neural Information Processing Systems*, 37: 100341–100368.
- Yao, Y.; Zhang, A.; Zhang, Z.; Liu, Z.; Chua, T.-S.; and Sun, M. 2022. CPT: Colorful Prompt Tuning for Pre-trained Vision-Language Models. *arXiv:2109.11797*.
- You, H.; Zhang, H.; Gan, Z.; Du, X.; Zhang, B.; Wang, Z.; Cao, L.; Chang, S.-F.; and Yang, Y. 2023. Ferret: Refer and Ground Anything Anywhere at Any Granularity. *arXiv:2310.07704*.
- Young, P.; Lai, A.; Hodosh, M.; and Hockenmaier, J. 2014. From image descriptions to visual denotations: New similarity metrics for semantic inference over event descriptions. *Transactions of the association for computational linguistics*, 2: 67–78.
- Yu, L.; Lin, Z.; Shen, X.; Yang, J.; Lu, X.; Bansal, M.; and Berg, T. L. 2018. MATTNET: Modular attention network for referring expression comprehension. In *Proceedings of the IEEE conference on computer vision and pattern recognition*, 1307–1315.
- Yuan, H.; Li, X.; Zhang, T.; Huang, Z.; Xu, S.; Ji, S.; Tong, Y.; Qi, L.; Feng, J.; and Yang, M.-H. 2025. Sa2VA: Marrying SAM2 with LLaVA for Dense Grounded Understanding of Images and Videos. *arXiv preprint arXiv:2501.04001*.
- Zhan, Y.; Zhao, H.; Zhu, Y.; Yang, F.; Tang, M.; and Wang, J. 2024. Griffon-G: Bridging Vision-Language and Vision-Centric Tasks via Large Multimodal Models. *arXiv:2410.16163*.
- Zhang, B.; Zhang, P.; Dong, X.; Zang, Y.; and Wang, J. 2024. Long-clip: Unlocking the long-text capability of clip. In *European Conference on Computer Vision*, 310–325. Springer.
- Zheng, K.; Zhang, Y.; Wu, W.; Lu, F.; Ma, S.; Jin, X.; Chen, W.; and Shen, Y. 2024. DreamLIP: Language-Image Pre-training with Long Captions. *arXiv:2403.17007*.
- Zhou, C.; Loy, C. C.; and Dai, B. 2022. Extract free dense labels from clip. In *European conference on computer vision*, 696–712. Springer.

More Evaluation Results

Due to space limitations in the main manuscript, we further present the experimental results for ViT-L/14 here. We tested and report PixCLIP’s performance on Instance-COCO and ImageNet-S.

The results for zero-shot region classification is shown as Table.7 and Table.8. The experiments effectively demonstrate that when provided with a foreground object mask through the alpha channel, our PixCLIP generates visual features that are more focused on the foreground object, leading to better image-level classification compared to the original CLIP and other baseline approaches. Notably, we followed the settings of Alpha-CLIP to enable MaskCLIP to accept task-specific formats. We also visualized and demonstrated PixCLIP’s leading performance over previous SOTA work AlphaCLIP on various benchmarks, as shown in Figure.5. Furthermore, we compared the indicators of our method with those of the most advanced approach on the fine-grained analysis benchmark. The results are shown in Table 10.

Methods	Input	Imagenet-S	
		Top1	Top5
ViT-B/16			
CLIP	C	66.48%	88.90%
MaskedAdaptedCLIP	C	57.86%	79.12%
Red Circle	VP	65.37%	88.68%
MaskCLIP	VP	67.86%	89.40%
Alpha-CLIP	VP	68.89%	90.51%
PixCLIP	VP	69.57%	91.17%
ViT-L/14			
CLIP	C	73.48%	91.60%
MaskedAdaptedCLIP	C	73.37%	92.09%
Red Circle	VP	77.04%	93.39%
MaskCLIP	VP	77.04%	93.39%
Alpha-CLIP	VP	77.41%	94.45%
PixCLIP	VP	79.42%	94.77%

Table 7: Accuracy comparison of zero-shot classification on **ImageNet-S**. The "C" in the table signifies models that take a mask’s corresponding **Cropped Image** as direct input. "VP" indicates that, in addition to the image, the model can also directly accept a **Visual Prompt**.

Detailed Setting

In this subsection, we list our model architecture and all parameters pertaining to the experimental setup. The detailed parameters are shown in Table 9.

Inference Stage

During training, we adopt a three-branch framework to train the visual encoder. In the inference stage, the visual encoder only requires the full image and the corresponding mask, without the need for cropping or extracting features from specific regions, as illustrated in Figure 6.

Methods	Zero-shot Classification	
	Top1	Top5
ViT-B/16		
CLIP	64.21%	86.69%
Alpha-CLIP	71.08%	88.90%
LLM2CLIP	70.16%	87.40%
PixCLIP	76.68%	90.56%
ViT-L/14		
CLIP	71.48%	90.15%
Alpha-CLIP	77.48%	94.40%
LLM2CLIP	xx.xx%	xx.xx%
PixCLIP	79.42%	94.77%

Table 8: Accuracy comparison on **Instance-COCO**.

Parameter	Value
Model Structure	EVA02
Backbone	ViT-B/16
Optimizer	AdamW
Learning Rate	1×10^{-5} (Mask Conv)
	1×10^{-7} (Other Layers)
α	0.25
β	0.25
Warm Up Length	800 steps
Train Epochs	8
Full Image Ratio	0.1
Adaptor Layers	4
Batch Size	128×8
AMP (bf16 training)	True
Clip Log Scale	4.0652
Weight Decay	1×10^{-2}

Table 9: Detailed List of Parameters for Model and Training

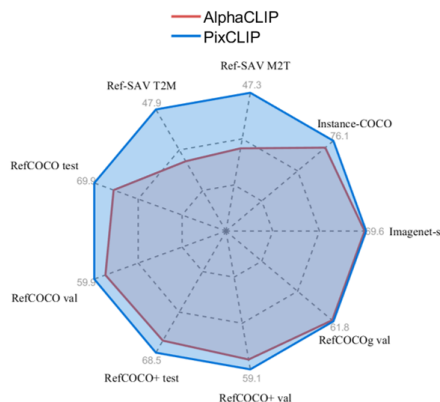


Figure 5: Performance comparison between PixCLIP and prior state-of-the-art works.

Model	MSCOCO		Flickr30k		Winoground		
	I2T	T2I	I2T	T2I	T.	I.	G.
<i>Model Architecture: ViT-B/16</i>							
DreamLIP	53.3	41.2	82.3	66.6	26.0	10.00	7.25
LiT	30.0	16.5	54.8	38.5	24.3	6.5	4.8
ShareLock	26.0	13.5	53.9	34.9	26.3	12.8	5.3
CLIP-B	55.4	38.3	83.2	65.5	25.7	11.5	7.75
SAIL-B-GTE	48.2	37.9	76.5	63.9	31.0	11.5	9.5
SAIL-B-NV2	57.3	45.3	84.1	70.1	35.0	17.25	13.0
PixCLIP	52.7	50.2	84.2	87.0	35.25	17.75	12.0

Table 10: Results on complex-reasoning and fine-grained tasks.

Broader Impact

Our PixCLIP model overcomes the limitations of traditional methods in vision-language tasks. While conventional models can only accept full image input and text inputs within a fixed length, our model can effectively and tightly align image regions of arbitrary granularity and texts of arbitrary length into the same feature space. We contribute to developing a coherent learning framework that enhances CLIP’s fine-grained capabilities and transferability. Simultaneously, we pioneer a new task, namely retrieval between image regions and text, and provide the LongGRIT dataset for benchmarking future models. To ensure a positive social impact, the data we use does not involve any personal privacy issues.

Limitation

PixCLIP still has two significant limitations: **(1)** Although we possess high-quality data, the size of data is insufficient, with only 1.5M samples, hindering effective scaling up. Future approaches might involve more extensive self-supervised training with larger amounts of unlabeled data or constructing more efficient data utilization pipelines. **(2)** When creating the LongGRIT dataset, we did not specifically consider hard negative samples—for instance, having MLLMs intentionally modify a core attribute in a correct description. Future work based on this direction might achieve higher data quality and more efficient data utilization by generating such samples.

More Visualization Results

Follow the previous works, we visualize PixCLIP’s attention maps to check whether our model pays more attention to user-defined highlighted areas at feature grid space. For a fair comparison, We check the attention map of [CLS] token in the last transformer block in the vision encoder.

Results are shown in Fig.7. This visualization verifies that our model pays more attention to the area to focus on and effectively learns to understand fine-grained semantics.

Additionally, we visualized our model’s fine-grained responsiveness to text when given a whole image as input. We computed an attention map by calculating the similarity between the feature map from our model’s last layer and the text features. Fig.8 presents our visualization results,

which demonstrate that our mask-guided input enhances local features when processing the entire image. We maintain a comparable performance level compared to previous fine-grained methods.”

More Examples For Data Generation

We provide some visualized examples of our LongGRIT, shown in Fig.3. Additionally, we showcase the features of our LongGRIT dataset through samples that demonstrate multi-granularity, occlusion reappearance, and both short and long text expressions. These features make LongGRIT also be a challenging and comprehensive **Mask-Text Retrieval** benchmark.

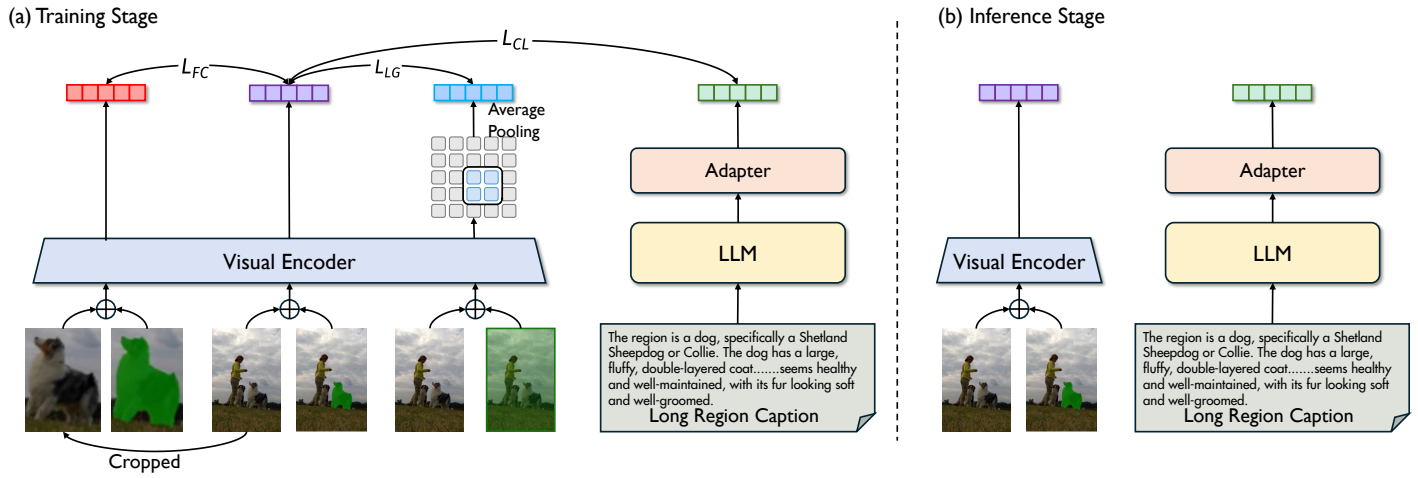


Figure 6: The distinction between PixCLIP at training time and inference time.

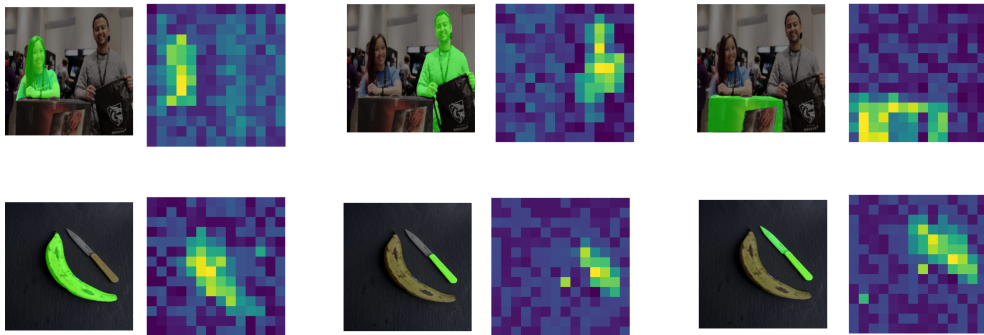


Figure 7: Visualized examples of attention map

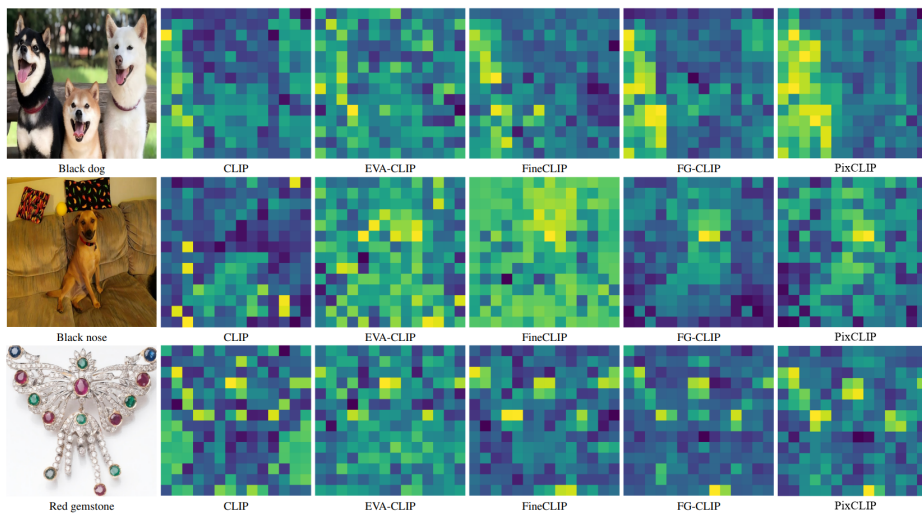


Figure 8: Visualized examples of attention map



The region features a fake wound or injury, likely used for educational or training purposes, and is located on the arm of a young girl with long, dark hair, wearing a blue uniform with a name tag. The wound looks realistic but is probably made from materials such as latex or silicone to simulate an injury. This kind of prop is often used in medical training, first aid courses, or film and theater productions to create a convincing visual effect. The girl is seated at a table with a red object on it, which appears to be a toy or a piece of equipment, and she is smiling and pointing at the camera, indicating that she is the subject of the photograph. The background is blurred, but it seems to be an indoor setting with other tables and chairs, suggesting a communal or educational environment.



The region features a young girl with a dark complexion, wearing a blue uniform with a name tag. She is seated at a table with a white surface, and her expression is one of surprise or shock. Her hair is pulled back, and she is wearing a headband. The table has a few items on it, including what appears to be a red object that could be a toy or a piece of equipment. The background is blurred, but it seems to be an indoor setting with other tables and chairs, suggesting a communal or educational environment.



The region features a person clapping hands and the region is located in the top-right part of the image. The person is wearing a hat and a blue shirt, and appears to be participating in a parade or public event. The man in the blue shirt is clapping his hands and appears to be engaged in the event. He has a relaxed posture and is standing in the middle of the crowd, suggesting he is a participant or an attendee at the event. The man's attire is casual, suitable for an outdoor gathering, and his hat suggests it might be a sunny day. The blue shirt he is wearing is a solid color, and the straw hat has a wide brim, which is typical for sun protection.



The object in the image is a person clapping their hands. The individual is wearing a black t-shirt with a graphic design, a baseball cap, and sunglasses. They appear to be at an outdoor event, as there are other people visible in the background. The man is the central figure in the image, wearing a black t-shirt with a graphic design and white shorts. He is clapping his hands in front of him, which is a gesture often associated with approval or celebration. His attire and the context suggest he is at a casual, outdoor event. The man's facial expression is not fully visible due to the angle of the photo, but his posture and the action of clapping are the most notable features in this region. The region is located in the center of the image.



The region contains a man who is playing a traditional Chinese instrument, the erhu, which is a traditional Chinese string instrument often referred to as the "Chinese violin." It consists of a long, narrow neck with two tuning pegs and a small, hexagonal soundbox covered with python skin. The musician plays the erhu using a bow, which is placed between the two strings. The erhu is known for its expressive and haunting sound, and it is commonly used in both traditional Chinese music and contemporary compositions. The man is wearing a red shirt and is seated at a table with the large. His performance attracted a woman and a man in the background to sit and watch him. The setting seems to be indoors with a window in the background showing a view of trees and a building. The region is in the upper right corner of the image.



The object in the image is a musical instrument known as a guzheng. The guzheng is a traditional Chinese stringed instrument with a long history, dating back over 2,500 years. It typically has 16 to 26 strings and is played by plucking the strings with the right hand while the left hand presses on the strings to change the pitch. The guzheng is known for its rich, resonant sound and is often used in Chinese classical music and folk music. The region is a musical instrument, specifically a traditional Chinese instrument known as a pipa. It is a four-stringed instrument with a long neck and a round body, which is being played by a person. The instrument is made of wood and has a dark brown color. The strings are white, and the instrument is held with both hands, with a woman's left hand pressing down on the strings to change the pitch and the right hand plucking the strings to produce sound. It is often used in classical and folk music performances. The region is located in the bottom-right part of the image.

Figure 9: Visualized examples of our LongGRIT.



The region features a coffin draped with the national flag of Iraq. The flag features three horizontal stripes of red, white, and black, with the Takbir (الله أكبر), "Allahu Akbar" or "God is the greatest" written in green Kufic script in the center of the white stripe. This type of flag-draped coffin is often used in military or state funerals to honor the deceased. The coffin is covered with a cloth that has a black background and white text, and it is the central focus of the image. The text is in Arabic and is the only text present in the image. The cloth is draped over the object, and the edges of the cloth are visible at the bottom of the image. The object itself is not fully visible, but it appears to be a flat surface, possibly a table or a platform. The cloth has a slight sheen, suggesting it may be made of a material like silk or satin. The text on the cloth is clear and legible, indicating that it is an important element of the image. The region is located in the center of the image.



The object in the image is a ripe banana, with a yellow color and a small brown spot. The banana is being held by a woman with her right hand, positioned in front of her and slightly to the left. The woman is wearing a light grey top and has long, dark hair. She is smiling and appears to be in a relaxed and happy mood, standing in a kitchen as the background. The region is located in the center of the image.



The object in the image is an ant. It is characterized by its small size, brown coloration, and the distinctive body shape of an insect, with a head, thorax, and abdomen. It is positioned on a branch, which is a common behavior for ants as they often traverse branches in search of food or to establish their territory. The ant's antennae are extended, which is typical for ants as they use their antennae for sensing their environment. The background is dark and out of focus, which helps to highlight the ant and the branch it is on. The region is located in the left of the image.



The region in question features a small, red beet slice. It is one of several slices that are scattered around the glass of beet juice. The slice is thin and has a smooth, slightly curved edge. The color is a vibrant red, consistent with the juice's hue, and it appears fresh and crisp. The red beetroot slices connect to the whole beets, juice, and wooden surface, illustrating the vegetable's fresh, natural versatility from raw to prepared. The region is located in the bottom right part of the image.



The region is a man, likely a public figure or politician. He is dressed in a dark suit and tie, which is typical attire for formal occasions or professional settings. His posture and the direction of his gaze suggest he is walking purposefully, possibly towards or away from the camera. The man's facial expression is serious, and he appears to be in mid-stride, indicating movement. The background is blurred, which is a common technique in photography to focus attention on the subject. The image does not provide enough detail to determine the man's exact identity or the specific location, but the presence of the camera and the formal attire suggest a setting of significance, possibly related to a public event or a formal engagement. The region is located in the bottom left part of the image.



The object in the image is a diving helmet, which appears to be an older model, possibly made of metal, with a round, bulbous shape and several ports or valves on the top. It is displayed among a collection of diving helmets and masks, with various designs, including both traditional and modern shapes, as well as a range of colors from metallic gold to dark brown. The helmets were displayed on a table with many other helmets, many of which had information boards on the front. It indicates that it is in an exhibit or a collection meant for public viewing. The region is located in the bottom left part of the image.

Figure 10: More visualized examples of our LongGRIT.

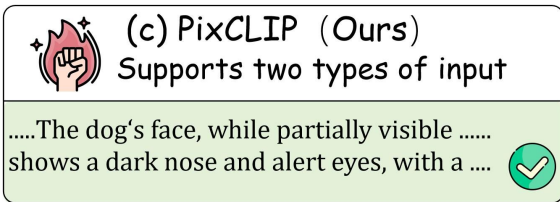
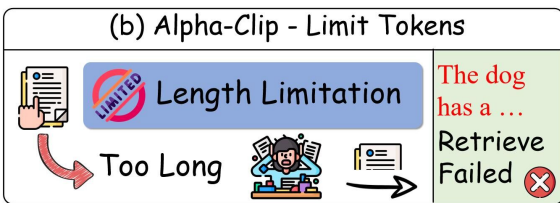
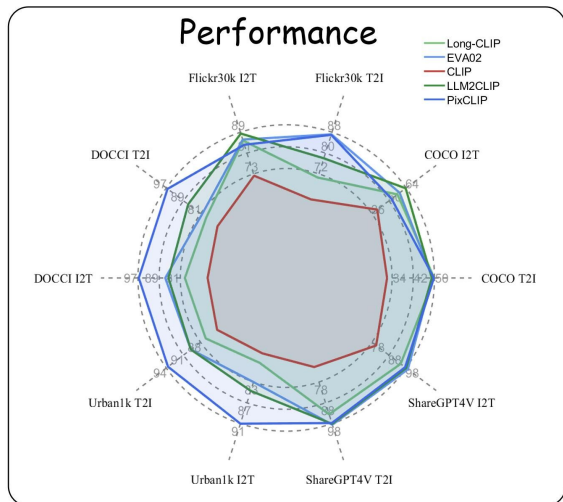
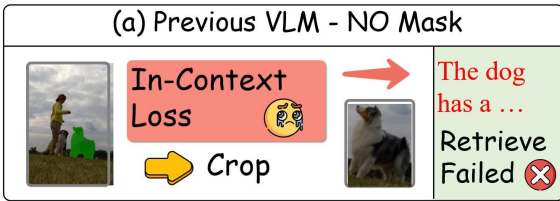
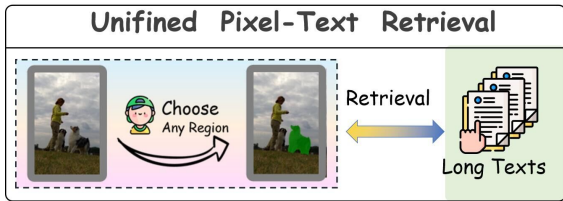


Figure 11: PixCLIP: Achieving Fine-grained Visual Language Understanding via Any-granularity Pixel-Text Alignment Learning.